

## DEVELOPMENT OF A COMPUTATIONAL TESTBED FOR NUMERICAL SIMULATION OF COMBUSTION INSTABILITY

Jeffrey Grenda\*, Sankaran Venkateswaran† Charles L. Merkle‡

Propulsion Engineering Research Center

and

Department of Mechanical Engineering

The Pennsylvania State University

University Park, PA 16802

### SUMMARY:

A synergistic hierarchy of analytical and computational fluid dynamic techniques is used to analyze three-dimensional combustion instabilities in liquid rocket engines. A mixed finite difference/spectral procedure is employed to study the effects of a distributed vaporization zone on standing and spinning instability modes within the chamber. Droplet atomization and vaporization are treated by a variety of classical models found in the literature. A multi-zone, linearized analytical solution is used to validate the accuracy of the numerical simulations at small amplitudes for a distributed vaporization region. This comparison indicates excellent amplitude and phase agreement under both stable and unstable operating conditions when amplitudes are small and proper grid resolution is used. As amplitudes get larger, expected nonlinearities are observed. The effect of liquid droplet temperature fluctuations was found to be of critical importance in driving the instabilities of the combustion chamber.

### TECHNICAL DISCUSSION:

Current understanding of liquid rocket combustion instability has been obtained through the implementation of two primary tools: experimental investigations and analytical models. Computational capabilities have recently advanced to the point where they provide a third potential investigative tool to complement these existing approaches. The dramatic progress in the field of computational fluid dynamics (CFD) over the past decade has demonstrated the ability to model highly complicated flow phenomena typical of combustion chambers. CFD methods offer a promising methodology to model not only the important subprocesses such as atomization and vaporization, but also to directly simulate and accurately capture the acoustical physics of the combustion chamber.

Research directed towards developing computational instability models for liquid propellant engines has been undertaken in several research groups. Early work using computational fluid dynamics in studying combustion instability was performed by Habiballah *et al.* [1] and Liang and Ungewitter [2], and followed later by Bhatia and Sirignano [3], Jeng and Litchford [4], Kim *et al.* [5], Wang *et al.*[6], as well as the current authors [7]. Typical results using these time-marching approaches have found that droplet size, mixture ratio, and mean chamber conditions are important physical parameters. Due to computational restrictions, most analyses have considered axisymmetric or

---

\*Graduate Research Assistant

†Research Associate

‡Distinguished Alumni Professor

annular geometries, although some preliminary three-dimensional results for a thin or “collapsed” combustion zone have previously been reported by the current authors [7].

The current work develops a computational testbed for modelling a distributed vaporization zone by coupling CFD with available empirical and semi-empirical models of the dominant subprocesses in rocket engines. These solutions are then compared with closed-form analytical solutions to verify their accuracy. Although the solution of the unsteady, three-dimensional fluid dynamic equations is straightforward in principle, the required computational resources limit the quantity of solutions that can be obtained. This is the motivation for providing companion analytical procedures, which may be performed in a significantly more efficient manner. This approach permits important trends in relevant physical variables to be identified rapidly while simultaneously allowing a systematic assessment of the numerical issues involved.

The unsteady Euler equations are used to describe the fluid dynamics of the three-dimensional gas phase flowfield within the combustion chamber. Due to the substantial computational cost associated with finite difference solutions of the three-dimensional unsteady equations, a mixed character finite difference/spectral method is employed to decompose the primary variable  $Q$  in the circumferential direction into a Fourier series. The vector  $Q$  is given as a truncated series  $Q = \sum_{m=0}^M [\hat{Q}_{m,c}(x, r, t) \cos m\theta + \hat{Q}_{m,s}(x, r, t) \sin m\theta]$  where  $\hat{Q}_{m,c} = (\hat{\rho}_c, \hat{\rho}u_c, \hat{\rho}v_c, \hat{\rho}w_c, \hat{e}_c, 0, 0, 0, 0, 0)^T$  and  $\hat{Q}_{m,s} = (0, 0, 0, 0, 0, \hat{\rho}_s, \hat{\rho}u_s, \hat{\rho}v_s, \hat{\rho}w_s, \hat{e}_s)^T$  are time-dependent functions of both the axial and radial finite-difference directions. A general equation governing the dynamics of the flowfield development in Fourier space can then be written as

$$\frac{\partial \hat{Q}_{m,T}}{\partial t} + \frac{\partial \hat{E}(\hat{Q}_{m,T})}{\partial x} + \frac{1}{r} \frac{\partial \hat{F}(\hat{Q}_{m,T})r}{\partial r} = -\frac{m}{r} \hat{G}(\hat{Q}_{m,T}) + \frac{1}{r} \hat{H}_{tot}(\hat{Q}_{m,T}) \quad (1)$$

where the vectors  $\hat{E}$ ,  $\hat{F}$ ,  $\hat{G}$ , and  $\hat{H}_{tot}$  are conservative flux vectors written in Fourier space [7]. The source term vector  $\hat{H}_{tot}$  contains the interphase coupling terms between the gas phase and liquid phase analyses including effects such as atomization, vaporization, and injector coupling. Representative vaporization models based upon the work of Priem-Heidmann and Abramzon-Sirignano are summarized in Table 1. These relationships are complicated nonlinear functions of the liquid and gas phase variables. Linearized versions of these expressions written in terms of an appropriate set of independent variables lead directly to a combustion response function for the instability. This combustion response function in turn allows analytical solutions to be obtained which may complement CFD approaches.

One appropriate set of functional variables governing the droplet vaporization rate can be written as  $\dot{m}'_{vap} = f(p, u, T_l)$  where  $T_l$  is the liquid droplet temperature. Since the pressure and velocity are fundamental flow quantities, the evaluation of the combustion response functions is greatly simplified if the liquid temperature fluctuation can be eliminated. By manipulating the vaporization expression and combining it with a linearized energy balance over the droplet surface, the two-parameter expression

$$\dot{m}'_{vap} = \bar{m}'_{vap} \left[ \alpha^* \frac{p'}{\bar{p}} + \beta^* \frac{u'}{\bar{u}} \right] \quad (2)$$

provides a relationship for the rate of vaporization from a liquid droplet with a fluctuating temperature as a function of the mean vaporization rate and the acoustic disturbances of pressure and velocity. The values of the complex linearization constants  $\alpha^*$  and  $\beta^*$  are determined from the conditions within the combustion chamber. It is sufficient to note here that it is expected that the values of  $\alpha^*$  and  $\beta^*$  will directly determine the stability of the combustor in the linearized case.

For a constant mean flow, a small amplitude version of Eqn. 1 can be solved analytically. When the vaporization zone is treated with physical models in the form of Eqn. 2, the problem can be reduced to an eigenvalue solution in

terms of the vaporization constants and mean flow parameters. The dispersion relationship for the eigenvalues are obtained by manipulating the equations of motion to provide a single wave equation in the chamber,

$$p'_{tt} + 2\bar{u}p'_{xt} + (\bar{u}^2 + \bar{c}^2)p'_{xx} = \bar{c}^2\bar{m}_v \left[ (\alpha^* \frac{p'_x}{\bar{p}} + \beta^* \frac{u'_x}{\bar{u}}) + (\alpha^* \frac{p'_t}{\bar{p}} + \beta^* \frac{u'_t}{\bar{u}}) \right] \quad (3)$$

where the subscripts denote differentiation with respect to the particular variable. This expression also holds in regions where the mean volumetric vaporization term  $\bar{m}_v$  vanishes. Substitution of the classical acoustic form of solutions for pressure and velocity produces a dispersion relationship of the form

$$k^2(\bar{u}^2 + \bar{c}^2) + k \left( -2\bar{u}\omega + \frac{i\beta^* \bar{c}^2 \bar{m}_v}{\bar{\rho}\bar{u}} - \frac{i\alpha^* \bar{c}^2 \bar{u} \bar{m}_v}{\bar{p}} \right) + \omega^2 - \bar{c}^2 \lambda + \frac{i\alpha^* \bar{c}^2 \bar{m}_v \omega}{\bar{p}} = 0 \quad (4)$$

Here,  $\lambda$  is the radial wavenumber, and  $k$  and  $\omega$  are the complex wavenumber and frequency, respectively. Once these have been determined, the oscillatory flow quantities which determine the stability behavior can be evaluated. In this way, the analytical solutions provide a valuable means of validating and complementing the more general nonlinear numerical approaches described earlier. This capability of plays an important role in establishing a validated testbed upon which more comprehensive physical modelling can be added.

## RESULTS:

First, we consider the analytical dispersion relationship presented in Eqn. 4 for a uniformly distributed vaporization process. For simplicity, we neglect droplet production processes and instead specify an initial droplet size of  $140\mu$  and a total mass flow rate of 5 kg/sec ( $H_2$  and LOX) entering the combustion chamber. This corresponds to a vaporization zone 95% of the length of the combustion chamber.

In the absence of droplet temperature fluctuations,  $\alpha^*$  and  $\beta^*$  are real and depend on droplet Reynolds number and gas static pressure. A typical stability map for the constant liquid temperature case is presented in Fig. 1. The stability plane for the distributed vaporization model includes both stable and unstable regions depending on the values of the vaporization coefficients  $\alpha^*$  and  $\beta^*$ . Positive contours indicate unstable growth of disturbances, and negative values indicate stable decay. The neutral stability curve is indicated by the dashed contour and separates the unstable and stable regions which are labelled U and S, respectively. For this typical example, unstable regions are centralized in the regions of positive  $\alpha^*$  and negative  $\beta^*$ . This indicates that both pressure and velocity are important in determining the stability although pressure effects may be more important under certain conditions.

The estimated ranges of the two vaporization models are indicated by the shaded regions on the stability plane. These values are approximated by allowing possible variations in the properties and other constant terms in the vaporization expressions. The locations of the Priem-Heidmann and Abramzon-Sirignano models indicate that both lie in the stable region of the stability domain. These predicted results indicate that the coupling of the vaporization process alone for constant temperature liquid droplets is insufficient to sustain pressure oscillations characteristic of combustion instability. Similar stable behavior has also been found for a wide range of operating conditions. These generalized results confirm our previous numerical findings [7] that droplet vaporization without temperature fluctuations cannot account for unstable growth of pressure oscillations.

When liquid droplet temperature is permitted to fluctuate, the linearization coefficients in Eqn. 2 become complex numbers since they are functions of the complex frequency eigenvalue. Since both the real and imaginary components of  $\alpha^*$  and  $\beta^*$  may be important, the stability diagram becomes a more complicated four-dimensional space. The overall result is that the presence of a temperature fluctuation drives both the Priem-Heidmann and Abramzon-Sirignano models more towards instability. Both stable and unstable modes are possible, depending on the physical operating conditions within the combustion chamber.

Although the effects of the gas phase and liquid phase flow variables are strongly coupled and not easily separated, experience has demonstrated that droplet diameter and droplet temperature are two critical parameters that influence stability behavior. Fig. 2 presents a stability contour which has been determined computationally by a parametric study of these variables. Here, we specify a total mass flow rate of 3 kg/sec with a mean chamber temperature of 3000 K and pressure of 40 atm. The triangular upper bound of the stability is determined by the constraint that the droplets must totally vaporize within the chamber. The neutral stability curve is again indicated by a dashed contour and separates the unstable and stable regions which are labelled U and S, respectively. The results indicate that smaller initial droplet sizes and colder initial droplet temperatures tend to result in destabilized combustor behavior.

In order to demonstrate the applicability of the two-zone analysis with fluctuating temperature droplets, the predicted analytical solution is compared with numerical results using a pure mode initial condition and tracking the temporal evolution of the flowfield in time. Fig. 3 presents a comparison of the analytical and numerical solutions for the gas phase pressure oscillation at the upstream centerline of the chamber for an initial droplet diameter and temperature of 130  $\mu$  and 130 K, respectively. Also shown is a comparison of the analytical and numerical predictions for the fluctuating liquid droplet temperature at a axial location one-fourth of the chamber length. The agreement is excellent for both cases.

The stability behavior of practical engines is often tested by bombing or pulsing the combustion chamber to induce pressure oscillations. The numerical pressure response to an pulsed initial condition can be validated by using the long-term analytically predicted growth rate. As shown in Fig. 4, the short-term temporal response contains a wide variety of modes within the chamber. In the long-term solution, however, we expect the most unstable mode (predicted by the analytical method) to dominate within the combustion chamber. Here, we have shown the pressure fluctuation at the upstream centerline of the combustion chamber. A comparison with the analytically predicted solution indicates that the growth rates correlate to within about 0.1%. It is evident that the numerical and analytical solutions demonstrate excellent agreement, thus validating the CFD results.

#### REFERENCES:

1. Habiballah, M., Lourme, D. and Pit, F., "A Comprehensive Model for Combustion Stability Studies Applied to the Ariane Viking Engine", AIAA-88-0086, AIAA 26th Aerospace Sciences Meeting, January 11-14, 1988, Reno, NV.
2. Liang, R., Ungewitter, R., "Multi-Phase Simulations of Coaxial Injector Combustion", AIAA-92-0345, AIAA 30th Aerospace Sciences Meeting, January 6-9, 1992, Reno, NV.
3. Bhatia, R., Sirignano, W., "A One Dimensional Model of Ramjet Combustion Instability", AIAA-90-0271, AIAA 28th Aerospace Sciences Meeting, January 8-11, 1990, Reno, NV.
4. Jeng, S.M. and Litchford, R.J., "Nonlinear Analysis of Longitudinal Mode Liquid Propellant Rocket Combustion Instability", AIAA-91-1985, AIAA/SAE/ASME/ASEE 27th Joint Propulsion Conference, June 24-27, 1991, Sacramento, CA.
5. Kim, Y.M., Chen, C.P., and Ziebarth, J.P. "Numerical Simulation of Combustion Instability in Liquid-Fueled Engines", AIAA-92-0775, AIAA 30th Aerospace Sciences Meeting, January 6-9, 1992, Reno, NV.
6. Wang, Z.J., Yang, H.Q., Pindera, M.Z., and Przekwas, A.J., "CFD Simulations of Nonlinear Acoustics in Liquid Rocket Combustors", Penn State Propulsion Engineering Research Center and MSFC Fourth Annual Symposium, September 9-11, 1992, MSFC, Huntsville, AL.
7. Grenda, J.M., Venkateswaran, S., and Merkle, C.L., "Multi-Dimensional Analysis of Combustion Instabilities in Liquid Rocket Motors", AIAA-92-3764, AIAA/SAE/ASME/ASEE 28th Joint Propulsion Conference, July 6-8, 1992, Nashville, TN.

Model	Vaporization	Heat Transfer
Priem-Heidmann	$\dot{m}_{vap} = \pi d \bar{\rho} D Sh \ln \left[ \frac{p}{p-p_{v,s}} \right]$	$q_v = \frac{\dot{m}_{vap} \bar{c}_{p,v} (T_g - T_{d,s})}{e^{\beta^*} - 1}$
Abramzon-Sirignano	$\dot{m}_{vap} = \pi d \bar{\rho} D Sh^* \ln [1 + B_M]$	$q_v = \dot{m}_{vap} \left[ \frac{c_{p,l} (T_g - T_{d,s})}{B_T} \right]$

Table 1: Summary of Typical Vaporization Models

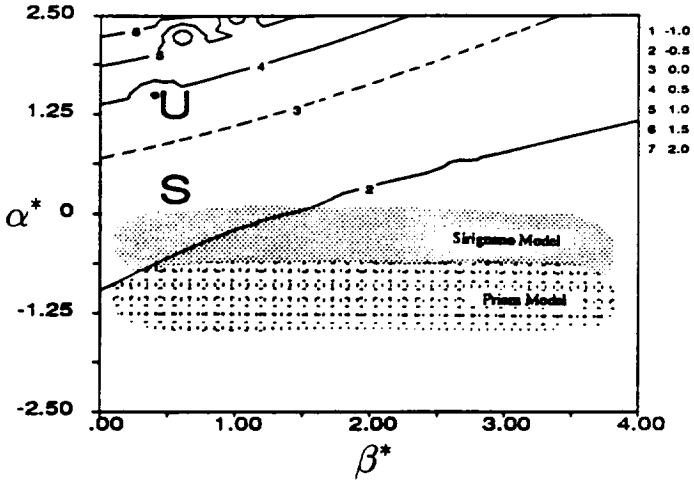


Figure 1: Distributed Vaporization Stability Plane; Constant Temperature Droplets With Initial Diameter 140μ; Most Unstable Growth Rate 1T,1R Instability Mode, Nondimensionalized Growth Rate.

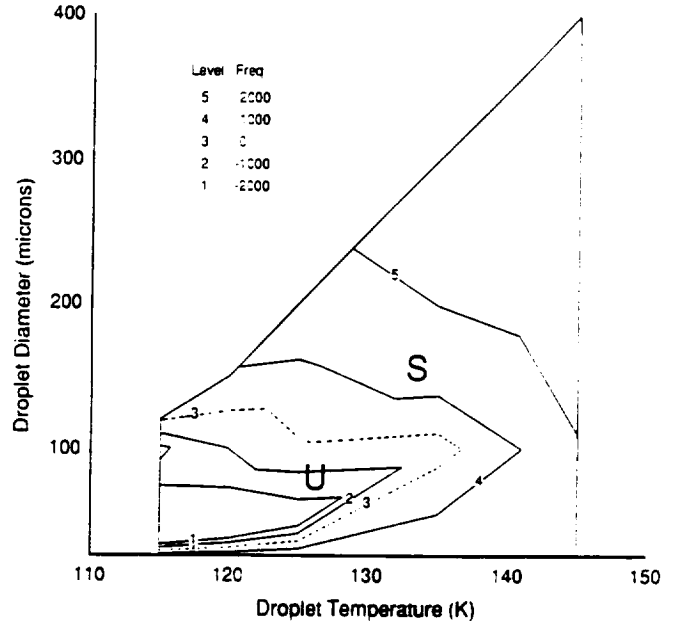


Figure 2: Distributed Vaporization Stability Plane as a Function of Droplet Diameter and Temperature; Variable Temperature Droplets; Most Unstable Growth Rate 1T,1R Instability Mode.

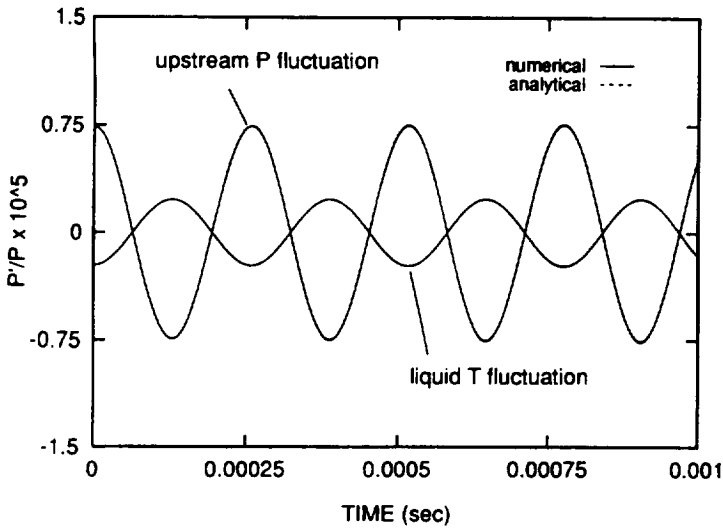


Figure 3: Pressure and Liquid Temperature Fluctuation vs. Time; Pure Mode 1T,1R Initial Condition.

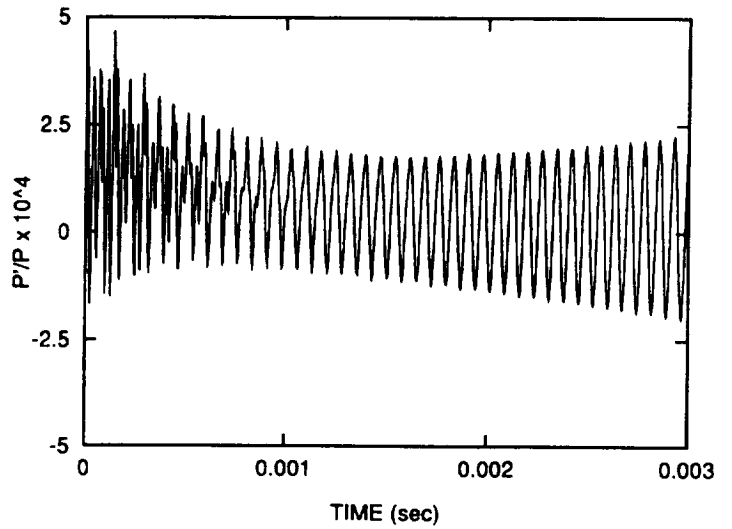


Figure 4: Upstream Centerline Pressure Fluctuation vs. Time; Pulsed (Mixed) Mode Initial Condition.